Lab 2 Report

Kitticopter Control System

Safiya Mia

EEE3094S Control Systems Engineering

MXXSAF002

Mechatronics: Department of Electrical Engineering

October 21, 2024

Contents

1 Introduction

In Lab 2, the objective was to design and implement a proportional controller for the kitticopter system. This involved system identification through step response analysis to derive the system's transfer function and validate it against experimental data. The proportional controller was then tested to maintain altitude tracking within acceptable limits. While it provided a degree of control, limitations were identified, including overshoot, settling time, and robustness under disturbances. These constraints highlighted the need for further optimisation to enhance the system's performance.

Building on the insights from Lab 2, Lab 3 focuses on compensator design. The primary aim of this lab is to improve the system's performance by implementing a first-order compensator. Unlike the proportional controller, the compensator offers greater flexibility in tuning system dynamics, such as reducing overshoot and improving setpoint tracking. Specifically, the compensator must meet stringent requirements, including a maximum overshoot of 20%, precise tracking to within 0.4m, and improved settling time based on system-specific parameters. The design leverages the controller circuits from Lab 2, which will be modified to form the new compensator.

Through simulation and physical testing, this lab aims to demonstrate the enhanced control capabilities offered by the compensator. The final report will evaluate the compensator's performance against set specifications, comparing it to the previous proportional controller, and exploring opportunities for further improvements in system stability and tracking accuracy.

Requirement	**Lab 2**	**Lab 3**
Overshoot (OS)	$\leq 30\%$	$\leq 20\%$
Tracking Accuracy	92% accuracy	Within 0.4m of final value
Settling Time	None	Settling time to 2% of final value within t_e
Disturbance Rejection	Not explicitly tested	Settle within t_e after disturbance
Sinusoidal Tracking	None	Track 0.1 rad/s sinusoid within 0.4m

Table 1: Comparison of Controller Requirements between Lab 2 and Lab 3

2 Controller Design

2.1 System Model and Controller Selection

The chosen controller was a lead controller which has a transfer function of

$$C(s) = K \cdot \frac{s-z}{s-p}$$

where $K = 1.3$, $z = -1.29937087$ and $p = -6.5331$.

The plant transfer function defined in Lab 2 is

$$G(s) = \frac{A}{s(\tau s + 1)} \tag{1}$$

where $\tau = 5.8165$ and $A = 21.084$.

A lead controller was chosen because it provides a straightforward yet effective way to improve the kitticopter's transient response, making it the easiest and most practical choice for this application. While a PD controller could also enhance transient performance by adding both proportional and derivative actions, it introduces additional complexity in tuning two parameters. In contrast, a lead controller achieves similar benefits—such as reduced overshoot, faster settling time, and improved stability—without the need for complex parameter adjustments. This simplicity, combined with its ability to meet the specifications (like sinusoidal tracking and precise disturbance rejection), makes it a more efficient option than other controllers.

2.2 Controller Design Process

2.2.1 Designing for Robustness

Although the provided lab instructions specify a settling time to 2% of the final value within 5 seconds and an overshoot of less than 20%, I aimed for more stringent specifications in my design. Specifically, I targeted:

- Settling time $\tau_{2\%} < 3.5$ seconds
- Overshoot $< 10\%$

Reducing the settling time ensures the system responds faster to changes or disturbances, which is essential for applications requiring quick adjustments. A faster response also minimises the time the system operates in transient mode, increasing stability and control. Lowering the overshoot reduces the risk of the system exceeding desired values, which can be especially critical for systems sensitive to overshooting. This minimises wear on components and prevents undesired oscillations. While the given specifications allow for a 20% overshoot, this may be too high for practical applications where precise control is desired. Designing with a stricter overshoot target aligns the system closer to industry standards, where minimising error is often prioritised.

2.2.2 Defining the Target Region of the S-Plane

The following calculations and diagrams illustrate the process of identifying the 'limiting poles' required to meet the specified settling time and overshoot criteria. These poles help define the restricted region on the root locus, guiding the controller design to ensure the desired system performance.

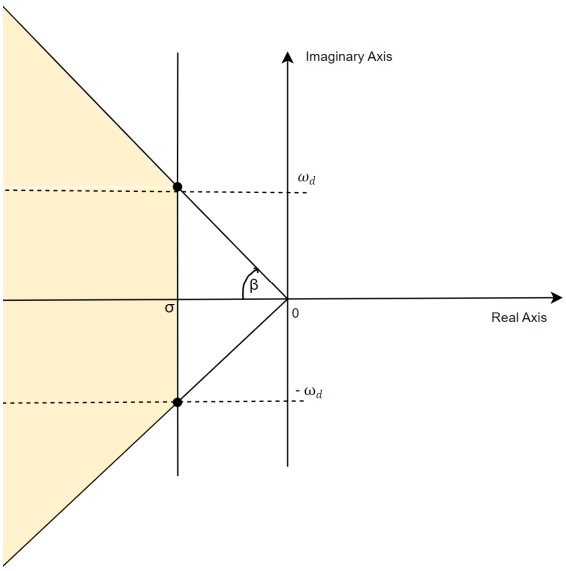

Figure 1: Target region (shaded) on the s-plane for the dominant closed-loop poles introduced by the compensator

The settling time specification is used to determine the value of σ, visually represented in Figure 1:

$$\tau_{2\%} < 3.5\,\text{s}$$
$$\Rightarrow 4\tau < 3.5\,\text{s}$$
$$\Rightarrow \tau < 0.875\,\text{s}$$

$$\sigma = -\frac{1}{\tau}$$
$$\Rightarrow \sigma = -\frac{1}{0.875}$$
$$\Rightarrow \sigma = -1.142857\,s^{-1}$$

The overshoot specification is used to determine the value of ω_d, visually represented in Figure 1. The formula for overshoot in terms of the damping ratio (ζ) is employed below:

$$OS = e^{\left(\frac{-\pi\zeta}{\sqrt{1-\zeta^2}}\right)} \tag{2}$$
$$\Rightarrow 10\% = e^{\left(\frac{-\pi\zeta}{\sqrt{1-\zeta^2}}\right)}$$

$$\Rightarrow \zeta = 0.591$$

The following relationship is used to determine the angle, β, from the damping ratio, ζ:

$$\beta = \arccos(\zeta) \tag{3}$$
$$\Rightarrow \beta = \arccos(0.591)$$
$$\Rightarrow \beta = 53.77^\circ$$

Finally, the right-angled triangle depicted in Figure 2 and derived from the s-plane in Figure 1 is used to calculate the value of ω_d using trigonometry:

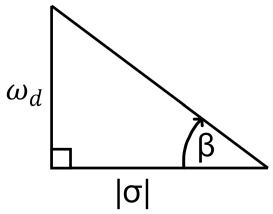

Figure 2: Right-angled triangle describing the relationship between σ, β and ω_d

$$\omega_d = |\sigma| \tan(\beta) \tag{4}$$
$$\Rightarrow \omega_d = |-1.142857| \tan(53.77^\circ)$$
$$\Rightarrow \omega_d = 1.5598 \text{ rad/s}$$

Thus, with reference to Figure 1, the s-plane locations of the limiting compensated poles are

$$s = \sigma \pm j\omega_d = -1.142857 \pm j1.5598$$

Due to the symmetrical nature of the complex conjugate poles, only the pole with the positive imaginary component, i.e. $s = -1.142857 + j1.5598$, will be referenced in future diagrams and calculations to simplify the analysis.

2.2.3 Calculating the Phase Lead

The open-loop poles of the system, defined by the transfer function in Equation 1, are located at 0 and $-\frac{1}{5.8165} = -0.17192$ on the Real Axis of the s-plane. This is visually represented below in Figure 3:

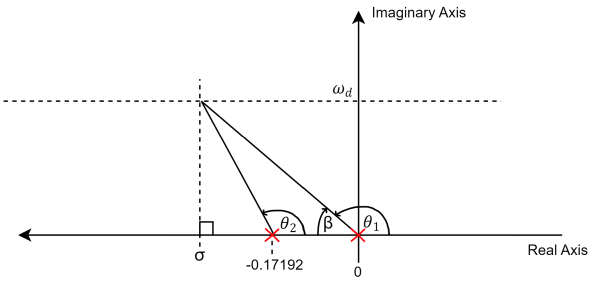

Figure 3: Root locus plot of the open-loop system poles

The phase at the desired limiting pole location, s = -1.142857 + j1.5598 is equal to

$$\Sigma \text{ angles from poles } - \Sigma \text{ angles from zeros,}$$

which is equal to

$$\theta_1 + \theta_2$$

(See Figure 3). Using the geometric relationships depicted in Figure 3:

$$\theta_1 = 180^\circ - \beta^\circ = 180^\circ - 53.77^\circ = 126.23^\circ$$

$$\theta_2 = 180^\circ - \arctan\left(\frac{\omega_d}{|\sigma - (-0.17192)|}\right) = 121.901^\circ$$

Since the open-loop system is marginally stable, the phase margin must be adjusted to ensure stability. The phase deficiency is:

$$\Delta\phi = -180^\circ + \theta_1 + \theta_2$$

$$\Rightarrow \Delta\phi = -180^\circ + 126.23^\circ + 121.901^\circ$$

$$\Delta\phi = 68.131^\circ$$

The required phase lead from the compensator is equal to the phase deficiency. Thus,

$$\phi_{lead} = \Delta\phi = 68.131^\circ$$

This is the amount of positive phase the compensator must introduce to achieve the desired performance.

2.2.4 Choosing a Location for the Zero

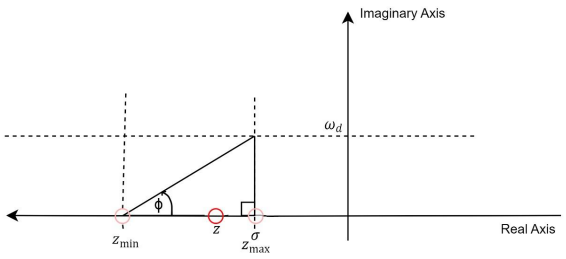

Figure 4: S-plane showing the possible locations for placing the zero of the lead compensator

To ensure that the zero does not affect the preferred settling time,

$$z_{\max} = -1.142857 s^{-1}$$

$$\tan(\phi) = \frac{\omega_d}{|z_{\min} - z_{\max}|}$$

$$\Rightarrow z_{\min} = -\frac{\omega_d}{\tan(\phi)} + \sigma$$

$$\Rightarrow z_{\min} = -\frac{1.5598}{\tan(68.131^\circ)} - 1.142857 = -1.768912 s^{-1}$$

Thus, the range of z is:

$$-1.768912\, s^{-1} < z < -1.142857\, s^{-1}$$

Choosing a zero that is safely within the range but closer to the imaginary axis for a better response:

$$z = \sigma - \frac{|z_{\min} - z_{\max}|}{4} = -1.142857 - \frac{|-1.768912 - (-1.142857)|}{4}$$

$$\Rightarrow z = -1.29937087\, s^{-1}$$

2.2.5 Calculating the Location of the Pole

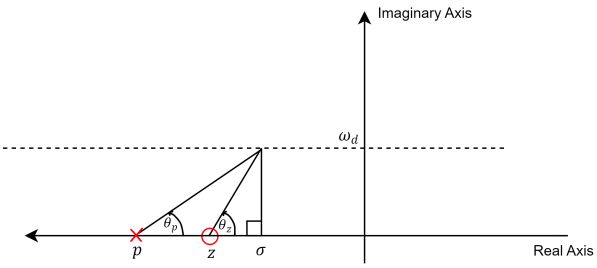

Figure 5: S-plane with annotations showing the geometric relationship between the compensated pole and zero

$$\theta_z = \arctan\left(\frac{\omega_d}{|z - \sigma|}\right) = \arctan\left(\frac{1.5598}{|-1.29937087 + 1.142857|}\right) = 84.27^\circ$$

$$\theta_p = \theta_z - \phi_{\text{lead}} = 84.27^\circ - 68.131^\circ = 16.139^\circ$$

$$\tan(\phi) = \frac{\omega_d}{|p - \sigma|}$$

$$\Rightarrow p = -\frac{1.5598}{\tan(16.139^\circ)} - 1.142857$$

$$\Rightarrow p = -6.5331\, s^{-1}$$

2.2.6 Calculating the Gain

$$K = \frac{1}{G(s)C(s)k_s} \tag{5}$$

$$K = \frac{1}{G(-1.142857 + j1.5598)C(-1.142857 + j1.5598) \times 0.61} = 1.143887791 \angle -180^\circ$$

A slightly higher gain of 1.3 is chosen to ensure that the response will lie on the roor locus within the target range of the s-plane.

2.2.7 Circuit Schematic

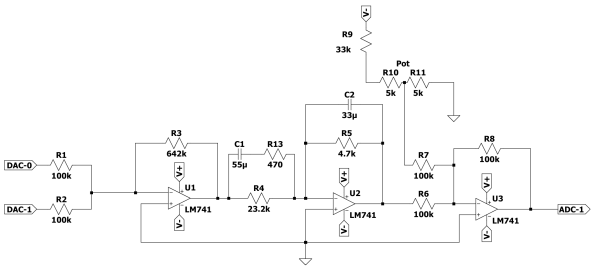

Figure 6: Lead Compensator Final Circuit Schematic

2.2.8 Calculating Resistor and Capacitor Values

$$R_4 C_1 = \frac{1}{|z|}$$

$$\Rightarrow R_4 = \frac{1}{|z| \times C_1} = \frac{1}{1.29937087 \times 33\mu}$$

Choosing the E12 capacitor value, $C_1 = 33\mu F$, yields $R_4 = 23321\Omega$ which can be approximated using the following E12 values: $\Rightarrow R_4 \approx 18k\Omega + 15.2k\Omega = 23.2k\Omega$

To confirm that the selected RC values, R_4 and C_1 do not produce a zero which is out of the desired range at their maximum tolerances:

$$|z_{highest}| = \frac{1}{R_4 C_1} = \frac{1}{0.9R_4 \times 0.9C_1} = 1.7612$$

$$|z_{lowest}| = \frac{1}{R_4 C_1} = \frac{1}{1.1R_4 \times 1.1C_1} = 1.1411$$

Thus, at their absolute worse, the chosen RC values will still introduce a zero that will not disrupt the desired settling time and overshoot.

Similarly C_2 and R_5 are selected:

$$R_5 C_2 = \frac{1}{|p|}$$

Choose $C_2 = 33\mu F$.

$$\Rightarrow R_5 = \frac{1}{|p| \times C_2} = \frac{1}{6.5331 \times 33\mu}$$

Choosing the E12 capacitor value, $C_2 = 33\mu F$, yields $R_5 = 4638\Omega$ which can be approximated using the following E12 value:

$$\Rightarrow R_5 \approx 4.7k\Omega$$

To reduce the effect of noise in the circuit, a resistor that is 10 times smaller than R_5 is placed in series with C_1, i.e. R_{13} is a 470Ω resistor.

Following the circuit configuration, the gain of the first op-amp stage is given by $\frac{R_3}{R_2}$ and the gain of the second stage is given by $\frac{R_5}{R_4}$. Thus, the total circuit gain is given by the following equation:

$$K = \frac{R_3}{R_2} \cdot \frac{R_5}{R_2} \tag{6}$$

Given that R_2 is set at $100k\Omega$ and using the value of K = 1.3 (chosen in section 2.2.6), yields a value of $641.7k\Omega$. This can be approximated using two E12 resistors in series: $560k\Omega$ and $82k\Omega$.

To confirm the actual gain of the circuit using the nominal resistor values, Equation 6 is used again:

$$K = \frac{560 + 82}{100} \cdot \frac{15 + 8.2}{4.7} = 1.3$$

This is an acceptable gain value which will be further validated in the following subsections.

2.2.9 Confirmation of Calculations Using MATLAB's Control System Designer

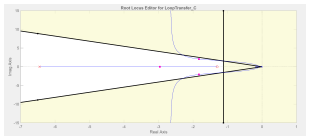

Figure 7: Control System Designer's Root Locus Analyser

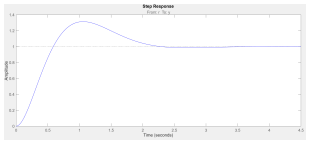

Figure 8: Control System Designer's Predicted Step Response

From Figures 7 and 8, it appears that the chosen compensator pole and zero lie within the target range of the s-plane, defined in Figure 1. The step response appears to have a settling time of less than 3 seconds and an overshoot of less than 10%.

2.2.10 Confirmation of Circuit Feasibility for chosen Gain Using LTspice

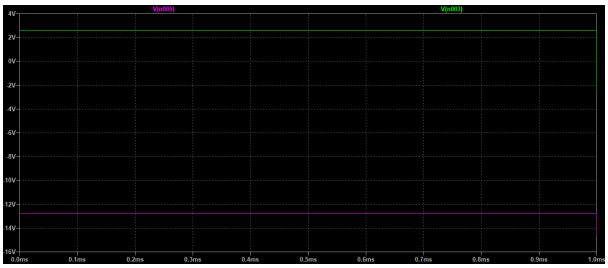

Figure 9: Op-amp gain analysis on LTspice

In Figure 9, the pink line represents the gain after the first op-amp stage. The green line represents the gain after the 2nd op-amp stage, which is the total gain of the controller, given that the third op-amp stage is designed to have unity gain. The circuit in Figure 6 was inputted with 1 volt via the DAC-0 and DAC-1 line and the op-amps were supplied with ± 15 volts. Because the controller sums the two inputs at the first stage in an inverting configuration, a gain of $2 \times \frac{642}{100} = 12.84$V is expected - this closely aligns with the pink line in the figure. Twice the total gain is expected at the output of the 2nd op-amp, so approximately $2 \times 1.3 = 2.6$ is expected. The total gain appears to be quite accurate following the green like in the figure.

3 Controller Testing

3.1 Simulink Testing

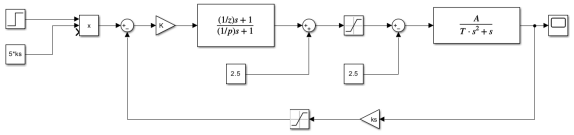

Figure 10: Complete model of the system with compensator in MATLAB Simulink

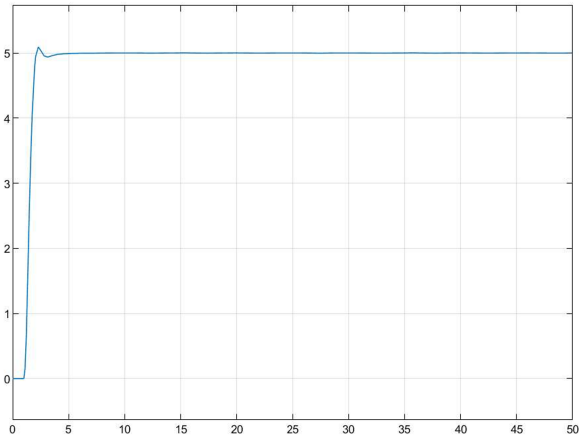

Figure 11: Simulated Step Response

From Figure 11, the approximate settling time is around 2.136 seconds. This indicates the time it takes for the system to stabilize within 2% of the final value. The graph shows that the response reaches the target with minimal oscillations, confirming that the compensator effectively improves settling time compared to the proportional controller. From Figure 11, the maximum overshoot is approximately 5.094 - 5 = 0.094 m, which is just under 2% of the setpoint. This minor overshoot shows that the compensator maintains control within the required 20% overshoot limit, reflecting improved transient performance.

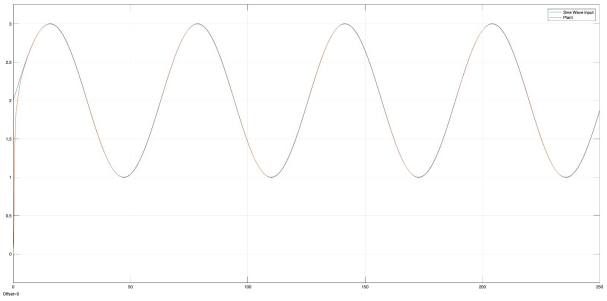

Figure 12: Simulation showing sinusoidal tracking of a 0.1rad/s sine wave

Figure 12 displays the system's response to a sinusoidal input at 0.1 rad/s. Both the sine wave input (blue line) and the plant's output (red line) are closely aligned, indicating that the compensator can track dynamic inputs with high precision. The minimal phase lag and amplitude deviation between the input and output confirm that the compensator meets the sinusoidal tracking requirement, keeping the error within the required 0.4m tolerance.

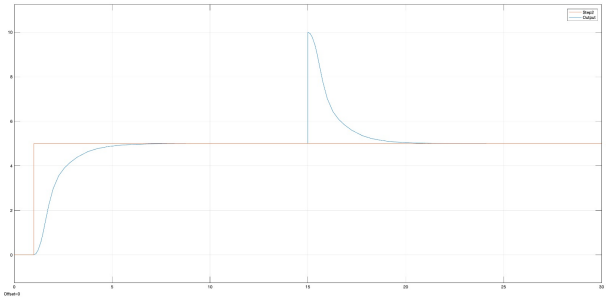

Figure 13: Simulation showing disturbance rejection within desired settling time

Figure 13 illustrates the system's ability to reject disturbances effectively. Initially, the output (blue line) follows the setpoint (red line), and a sudden disturbance is introduced, causing a spike around 15 seconds. The system quickly responds and returns to the original setpoint value, demonstrating excellent disturbance rejection. The settling time is well within the required limit of 5s, indicating that the compensator stabilises the system efficiently after disruptions.

3.2 Lab Testing

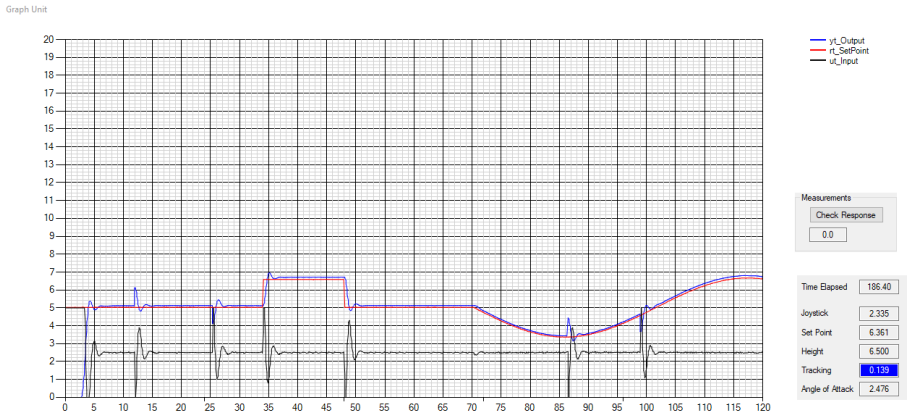

Figure 14: Final Demonstration Lab Performance

Initial Step Response and Setpoint Tracking (t = 0s to $\tilde{3}$4s):
The initial setpoint is 5 meters (as indicated by the red line). The system output (blue line) accurately tracks this value with a minor overshoot but quickly stabilizes at 5 meters, satisfying the overshoot requirement (well within the 20% limit). The system demonstrates stable tracking here, showing no significant oscillations and confirming that the

compensator ensures accurate and reliable step response.
Step Disturbance Response (t = $\tilde{3}$4s to $\tilde{4}$7s):
At around 34 seconds, a disturbance is introduced, causing the output to rise above 6 meters for a brief period. However, the system quickly rejects the disturbance, and by 47 seconds, the output has returned to the setpoint of 5 meters. This behavior demonstrates the disturbance rejection capability of the controller, which brings the system back to within 2% of the desired setpoint in a short amount of time. Around 70 seconds, the red line begins to follow a sinusoidal pattern. The output (blue line) tracks this sinusoid closely, staying within 0.4 meters of the sinusoidal setpoint, meeting the sinusoidal tracking requirement. This smooth tracking confirms the compensator's ability to handle dynamic inputs accurately. Throughout the demo, any overshoot is minimal and remains well below the 20% overshoot limit. The step responses settle quickly, with the output stabilising within the required 5-second settling time window after setpoint changes, meeting the settling time requirement.

3.3 Alignment between Simulations and Demo Results

The simulation results closely align with the demo performance, confirming that the compensator design is both accurate and robust across various conditions.

Disturbance Rejection In both the simulation (13) and the demo (between $t = 34s$ and $t = 47s$), the system demonstrates effective disturbance rejection. The simulation shows that after a disturbance spike, the system quickly returns to the desired setpoint within the required settling time, which mirrors the demo's recovery to the 5m setpoint after the introduced disturbance. This alignment validates the compensator's ability to reject disturbances efficiently under real-world conditions.

Sinusoidal Tracking The simulation (12) tracking of the 0.1 rad/s sinusoid aligns well with the sinusoidal response observed in the demo starting around $t = 70s$. Both the simulation and demo show minimal lag between the input and output signals, with the output closely following the input sinusoid. The system's ability to maintain tracking within the $0.4m$ tolerance in both cases confirms the compensator's effectiveness in handling dynamic inputs.

Overall System Behavior The smooth transition and stability demonstrated in the step response tests are consistent across both the simulation (11) and the demo. Minimal overshoot, fast settling times, and stable tracking performance observed in both contexts indicate that the compensator operates as expected, both in simulation and in practical testing.

These results demonstrate that the simulations were a reliable predictor of real-world performance, validating the compensator design and confirming that it meets all the specified performance criteria in both controlled and practical environments.

4 Performance Evaluation and Recommendations

In this lab, a lead compensator was designed and implemented to improve the kitticopter's control system performance. Compared to the proportional controller used in Lab 2, the compensator demonstrated better transient response, reduced overshoot, faster settling times, and enhanced disturbance rejection. The system successfully tracked both step and sinusoidal inputs within the required tolerances, meeting all specified performance metrics.

The results confirmed the effectiveness of the lead compensator in addressing the limitations identified in the previous lab. Additionally, the robust disturbance rejection and accurate sinusoidal tracking validate the compensator's suitability for dynamic environments.

To further enhance the performance of the system, several improvements can be considered. First, finer tuning of the lead compensator parameters, particularly the phase margin and gain, could help minimize overshoot and improve the settling time, especially during sudden disturbances. Second, replacing existing components with higher-precision resistors and capacitors would reduce variability in gain and phase shifts, leading to more consistent performance across multiple tests. Third, implementing low-pass filters in the input and feedback paths could reduce noise, which would stabilize the output further, particularly when tracking dynamic inputs like sinusoids. Lastly, testing the system under more extreme disturbances or larger step changes would provide additional insights into the limits of the compensator's performance and highlight further opportunities for optimisation.

5 Appendix and Notes

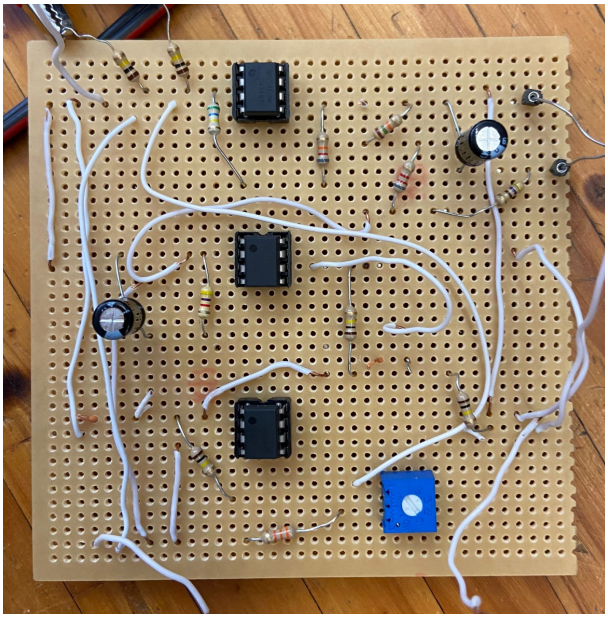

Figure 15: Final Lead Controller Circuit Soldered to a Veroboard